**JOURNAL OF THEORETICAL AND APPLIED MECHANICS**
**46**, 4, pp. 917-931, Warsaw 2008

# ELASTIC WAVE PHASED ARRAY FOR DAMAGE LOCALISATION

Wiesław Ostachowicz

*The Szewalski Institute of Fluid-Flow Machinery Polish Academy of Sciences, Gdansk, Poland*
*Gdynia Maritime University, Faculty of Navigation, Poland*
*e-mail: wieslaw@imp.gda.pl*

Tomasz Wandowski
Paweł Malinowski

*The Szewalski Institute of Fluid-Flow Machinery Polish Academy of Sciences, Gdansk, Poland*
*e-mail: tomaszw@imp.gda.pl*

In this paper, a problem of piezoelectric transducers used for damage localisation in an aluminium plate is investigated. Waves propagate in a specimen and reflect from boundaries and from discontinuities. Because damage reflected signals very often have a low amplitude, a phased array concept is utilized to amplify the signal. The amplification is based on the wave interference phenomenon. The star configuration consists of four linear phased arrays. As a result, a damage map is created combining four outputs of linear phased arrays. Several configurations with a varying number of transducers are investigated. The resulting damage maps are compared so as to balance the number of transducers and the possibility of flaw localisation using these maps. The presented investigation has only a numerical character.

*Key words:* phased array, Lamb waves, damage localisation

## 1. Introduction

Wave-based structural health monitoring is a non-destructive approach to ensure safety of structures. Especially skin panels of airplane fuselages are here an object of interest. Permanently attached piezoelectric transducers PZT (lead zirconate titanate) serve as a source of elastic waves and also as their sensor. Elastic waves in the form of Lamb waves in thin walled structures are very

sensitive to various discontinuities such as cracks, regions of corrosion, delaminations and matrix cracking (the last two for composite materials). Such discontinuities must be detected and localised in an early stage of development before they can hazard lives of airplane crew and passengers. Therefore, this subject is under investigation by many researchers (Deutsch *et al.*, 1997; Fomme *et al.*, 2004; Greve *et al.*, 2005; Peil and Loppe, 2006; Zhongqing *et al.*, 2006). Various configurations have been studied for damage localisation such as distributed placement of four PZTs for crack identification (Ye *et al.*, 2006) or clock-like manner sensor array (Zak *et al.*, 2006). In this paper a star configuration for damage localisation is investigated.

## 2. Specimen and elastic waves

A damage localisation procedure is conducted on a flat square aluminium panel (1000 mm×1000 mm×10 mm). Lamb wave propagation in this simple structure has been modelled by Spectral Element Method (Zak *et al.*, 2006) (40 × 40 elements, 36 nodes per element). The excitation and registration of waves in the specimen is realized in nodes of the Spectral Elements. The applied excitation signal (Fig. 1) has been chosen as a wave packet (5-cycle 100 kHz sine modulated with a Hanning window). It allows one to concentrate the excitation signal energy in a narrow frequency band.

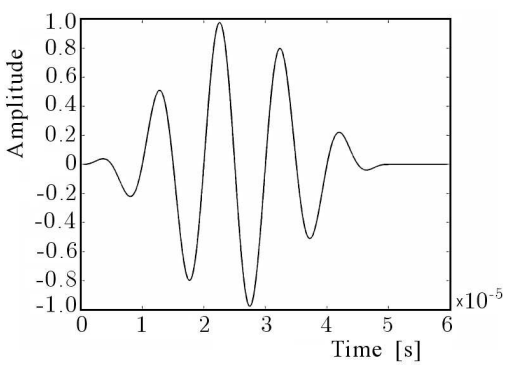


Fig. 1. Excitation Signal – 5-cycle 100 kHz sine Hanning window modulated

Generally, when piezoelectric transducers are used to generate waves in plates, both symmetric $(S_0, S_1, S_2, \ldots)$ and anti-symmetric $(A_0, A_1, A_2, \ldots)$ modes exist and the number of these modes depends on the product of the excitation frequency and the plate thickness. There are only two fundamental

modes, $A_0$ and $S_0$ (Fig. 2), that propagate up to almost 2 MHz·mm in aluminium. Therefore, the chosen frequency of excitation ensures that none of the higher modes will propagate in the specimen, which surely would make the signal analysis more difficult. The numerical model used allows analysing only propagation of the fundamental anti-symmetric Lamb wave mode $(A_0)$.

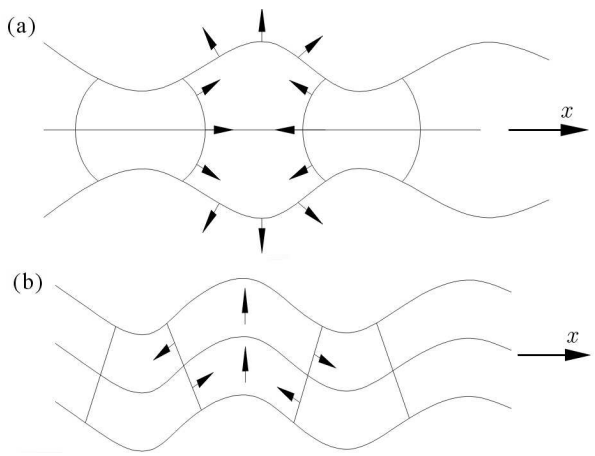


Fig. 2. Fundamental Lamb wave modes: (a) symmetric $S_0$, (b) anti-symmetric $A_0$

As it will be shown in Section 6, the wave group velocity $c$ is essential for the signal processing algorithm presented in this paper. Few numerical experiments have been conducted to determine the value of $c$. The average value of the Lamb wave mode $A_0$ group velocity resulting from these experiments is $c = 2777\,\mathrm{m/s}$.

## 3. Linear phased array theory

Linear phased arrays (Shi-Chang and Yijun, 1999; Purekar and Pines, 2001; Giurgiutiu and Bao, 2004; Sundararaman *et al.*, 2005; Pena *et al.*, 2006) are made of a certain number of piezoelectric transducers placed along a line at the same distance between each other. It is assumed that waves generated by the transducers have an omni-directional character and create a pattern, which is a result of superposition of the waves generated by each transducer individually. A sweep beam, which can be steered, is created if each transducer from the set excites waves with an individually adjusted time delay (Fig. 3). Changing the steering angle from 0 to 360° and calculating the time delay for

each transducer, an area of the structure around the array of transducers can be interrogated. This concept is known from radars, where the dish sweeps the space with a focused ray for target searching. When the waves from the radar find an object, they (the waves) are reflected from it and they return with some time delay. If the velocity of the wave generated by the radar and the angle of turn of the radar dish are known, then the position of the object can be determined by simple calculations. This technique is also used in damage detection but instead of a rotating radar dish, phased arrays are used for the beam-forming procedure. The principle of work of a phased array is explained below.

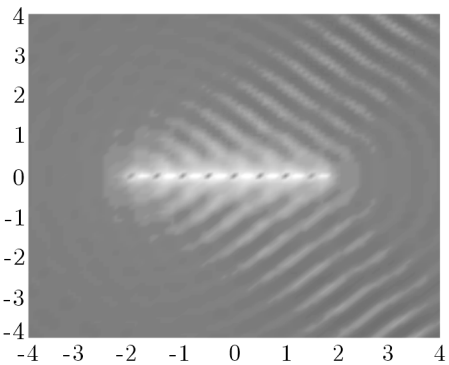


Fig. 3. Simulation of wave front creating for 16 transducers with spacing equal to the half wave length

Let us consider a set of $n$ transducers that can generate and receive elastic waves with an omni-directional character. Furthermore, it is assumed that the rays from the transducers are parallel. This assumption is justified only if the transducers are placed close to each other and the discontinuity causing wave reflection is far enough from the array. The greater the distance between the transducers the farther the discontinuity should be to make the idea of beam-forming useful. The beam-forming procedure is based on the signal interference principle. The procedure of producing a wave front can be divided in two cases: for a signal transmitted and for a signal received (Giurgiutiu and Bao, 2004). In order to focus the total signal in the direction indicated by the angle $\theta$ (Fig. 4), the $i$th array element should excite a wave with an individual time delay $t_i$ relative to the 1st PZT (Fig. 4), given by the formula

$$t_i = \frac{l_i \cos\theta}{c} \tag{3.1}$$

where $l_i$ is the distance between the $i$th and the 1st transducer and $c$ is the wave group velocity. The same procedure must be repeated for the signals

arriving to the sensors, which are backscattered from any obstacles situated at an angle $\theta$ because the ninth transducer is closer than the first one to discontinuities at the angle $\theta$.

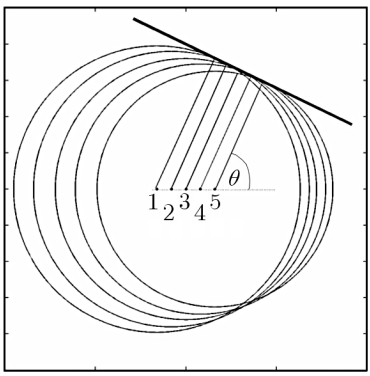


Fig. 4. Wave front creation principle

The focusing may be realized in two ways: electronically (an electronic system can excite waves with individual time delays) or by a computer algorithm (all transducer excite waves individually and signal processing procedures based on time shifting are applied to the gathered signals). The angle $\theta$ is changed from 0 to 360° and as a result the wave is amplified at angles corresponding to obstacles and faded for the rest.

## 4. Phased array algorithm

In this paper, results of numerical simulations are only discussed and the focusing of the beams is performed by a computer program as explained in the previous section. In this numerical simulation, waves are generated and registered by each transducer of the phased array.

The process of wave generation and sensing is conducted in $n$ steps. At each step, one transducer generates waves which are registered by all transducers. For the $n$th element phased array this makes a total of $n^2$ signals. Then a signal processing procedure is applied, which relies on time shifting for each collected signal with a time delay related to the spacing of transducers and the angle at which the beam is created. Signals registered in all sensors, when the excitation comes from the first transducer, are shifted in time to this transducer and then summed. In the next step, the same procedure is

repeated for the second transducer. This procedure is repeated for each sensor of the array. As a result, $n$ signals are obtained. This is how the beam-forming procedure for generating waves is carried out.

Similar operations are performed for the beam-forming procedure for the arriving signals. This can be achieved by shifting all the $n$ signals to the chosen transducer and summing them. This transducer is the point of origin for a virtual sweep beam.

Due to the discrete character of all signals, the calculated time delay is divided by a time step resulting from the simulation and rounded (an integer number is needed) to obtain a number of points for the discrete time shift. The time delays are calculated for beam angles from 0 to $360^\circ$ with a chosen step.

The signals are then transformed from the time domain into a physical domain of the structure using formulas

$$x = R\cos\theta \qquad y = R\sin\theta \tag{4.1}$$

where $R = ct/2$, $t$ is the time and $(x, y)$ are coordinates of the investigated surface area.

It gives in effect a damage map in which the $z$ coordinate represents the amplitude of the signal. The used MATLAB® plot procedures interpolate the signals for the rest of angles. As a result, a three dimensional damage map covering the area of the investigated structure is created (Giurgiutiu and Bao, 2004; Yu and Giurgiutiu, 2005). Values on the $z$ axis represent the amplitude of the interrogating signal at the point $(x, y)$ of the structure. In order to facilitate the map analysis, the squared signals are plotted.

In order to extract the damage signature, a special signal processing algorithm is proposed.

It is assumed that the excitation signals and the damage reflected signals have similar features. Therefore, the features of the total signal reflected from the damage can be compared to the excitation signal. For this purpose, a signal processing procedure, which uses a virtual rectangular time window with the same length as the excitation signal is used. The time window is used to extract a portion of the total received signal and then, features from this portion of the signal are compared to the excitation signal (Fig. 5). A similarity measure of the received signal portion and the excitation signal for a given point was built as a product of the absolute values of the excitation and the windowed signal portion and then summed for all points of the window. Based on this measure, a damage map can be plotted by applying the mentioned procedure for all points of the structural area under investigation. Damaged areas of the structure will have a high value of the similarity measure.

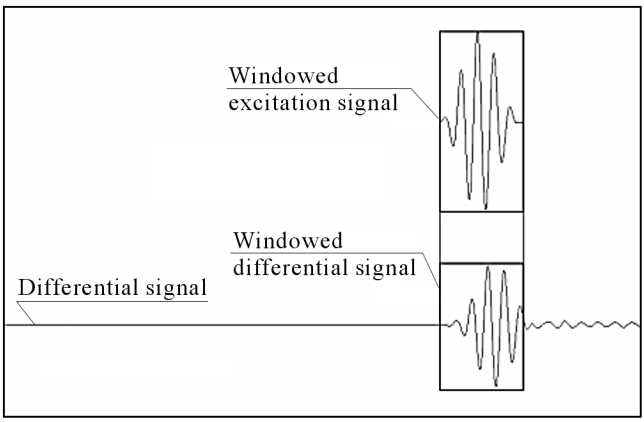


Fig. 5. Illustration of building a similarity measure for signal processing

## 5. Multi-phased array transducer configuration

In this paper, a combination of linear phased arrays is used (multi-phased array) forming a star configuration. The form of this configuration is an effect of authors, own research for the improvement of the ordinary linear phased array based damage localisation. The star configuration for 9 transducers in each linear array is presented in Fig. 6.

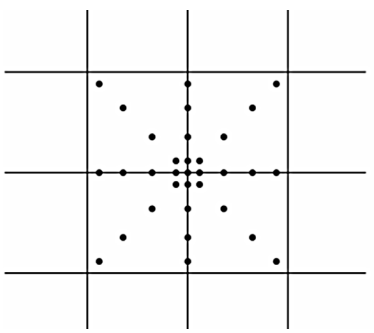

Fig. 6. Star transducers configuration

The distances between sensors/actuators are not equal, because this is how the nodes in the mesh of spectral elements are placed. The transducers have not been modelled; only the nodes are used as sources and receivers of waves. Four cases are considered and compared, for 3, 5, 7 and 9 transducers in a linear array. They correspond to 9, 17, 25 and 33 transducers in the whole configuration.

The beam-forming algorithm is independently applied to each array. As a consequence, four maps of the scanned area are obtained (Fig. 7). These maps are made of signals which represent the difference between the damaged and intact plate signals.

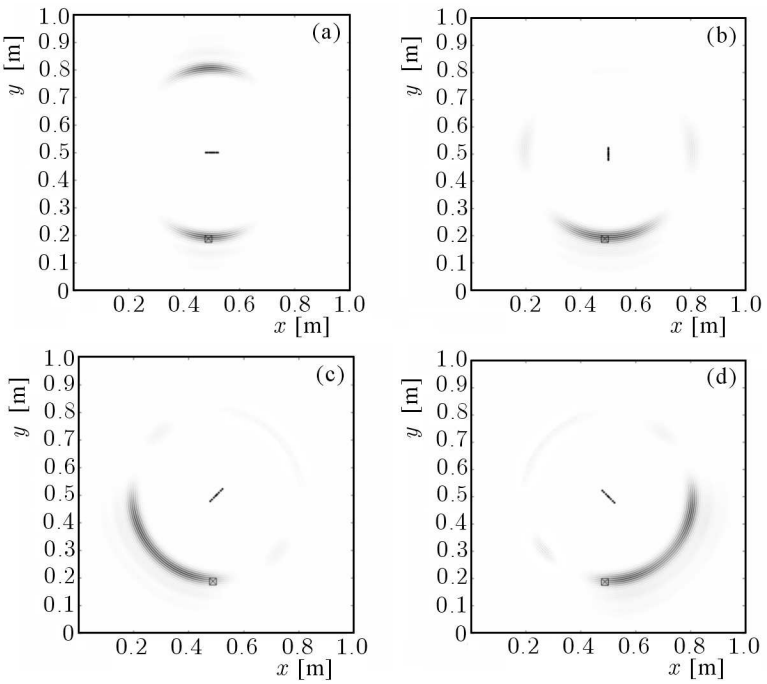


Fig. 7. Four component maps – the stripe in the middle represents an array for which the map is generated, black box indicates the simulated damage (90% stiffness reduction in one spectral element)

As can be noticed, the line on which the transducers from one array lie is a symmetry line of the map (Fig. 7). Therefore, a single map may indicate two damage areas (ghost damage) even if there is only one damage (Fig. 7a). This symmetry is even better seen on polar plots (Fig. 8) illustrating the amplitude (normalised to its maximum value) dependence on the angle. Figures 8a-d correspond to Figures 7a-d.

In order to remove the ambiguity of localization, an algorithm was proposed joining the four component maps into one (Fig. 9a). This final map is simply a product of the four component maps. It sharpens the image of damage more than the sum of the maps and allows a more precise localization of a defect than in the case of only one component map. A great advantage of this approach is also seen in Fig. 9b. The direction of the damage is indicated

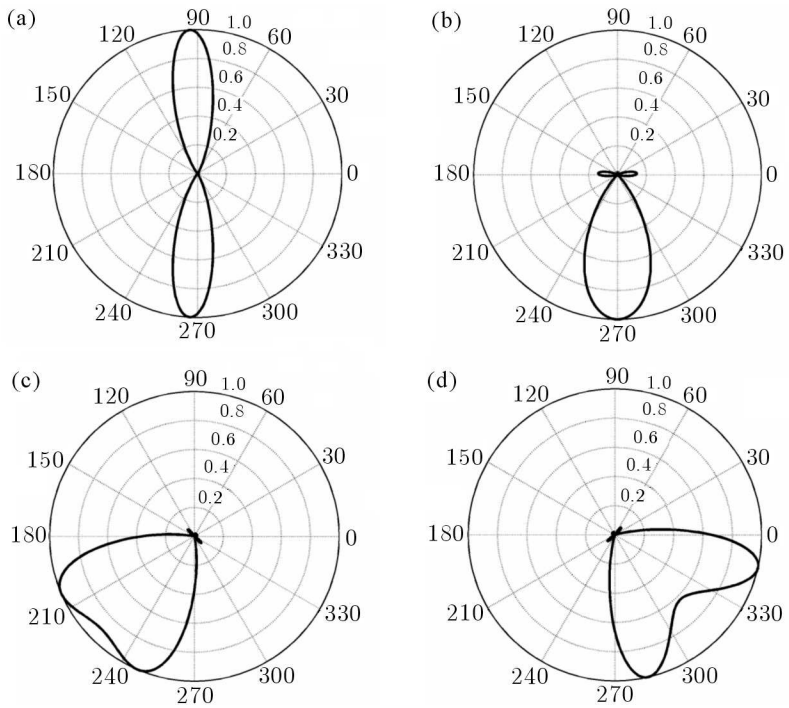


Fig. 8. Fig. 8 Amplitude angle dependence for four arrays (damage simulated as 90% stiffness reduction in one spectral element), (a) horizontally placed array, (b) vertically placed array (c) an array rotated by $45°$, (d) an array rotated by $-45°$

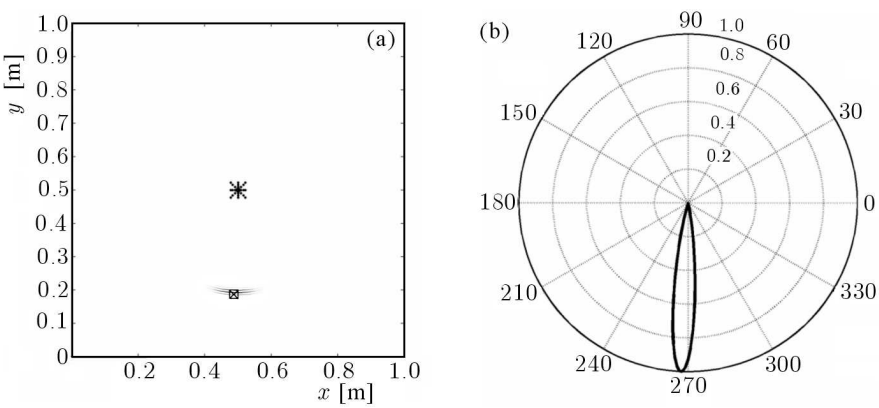


Fig. 9. Four maps joined for damage as a 90% stiffness reduction, (a) resulting map, (b) amplitude angle dependence

very precisely there. Comparing Fig. 9b with Fig. 8, one may observe that the proposed algorithm gives better results than any component map.

The above results (Fig. 7, Fig. 9a) show the localization of damage modelled as a 90% stiffness reduction in one spectral element. The scale of colours is linear from white (indicating the minimum level of the signal amplitude) to black (the maximum level of the signal amplitude).

Signals used for the damage map algorithm were corrupted with random noise (up to 10% of the signal amplitude) to make the investigation more related to real measurements.

## 6. Effect of transducers number

Investigation of the effect of the number of transducers on damage localization was begun with a simple damage scenario, namely one 25 mm long crack modelled as separation of the nodes between appropriate Spectral Elements. It is placed approximately at the angle 45° with respect to the plate centre, which is also the centre of PZT configuration used to localise the damage.

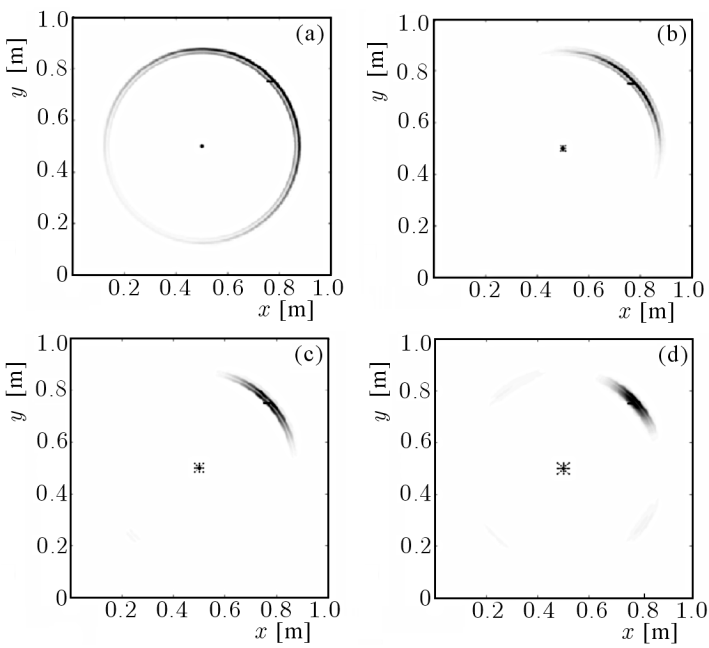


Fig. 10. Damage map for 25 mm long crack localisation for the case of: (a) 9, (b) 17, (c) 25, (d) 33 transducers in the star configuration

Figure 10 depicts the damage maps for this case. They correspond to 9, 17, 25,33 PZT transducers in the star configuration, respectively. One may notice that an increase of the number of transducers results in a decrease of the damage signature (the area where the signal is amplified by the algorithm). To study this result more precisely, polar plots are presented in Fig. 11, which correspond to the damage maps in Fig. 10. Polar plots show the amplitude dependence on the angle. The values of amplitude on these plots have been normalised in relation to the amplitude of the damage map for the 33-PZT configuration (Fig. 10d). Analysing Fig. 11, one may notice that adding the transducers to the star configuration causes that the direction of the crack becomes more apparent and precise. Although on the map (Fig. 10d) small additional increments of the amplitude appear (around points ($x = 0.4$, $y = 0.8$) and ($x = 0.8$, $y = 0.3$)), which may be also noticed on the corresponding polar plot (Fig. 11d), its amplitude is negligible. After this one-crack case, the plate with two cracks (25 mm both) has been investigated.

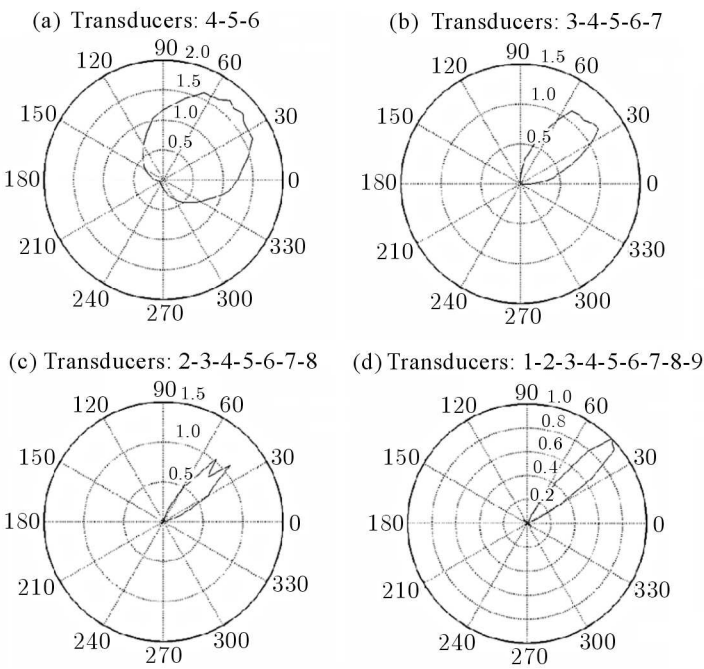


Fig. 11. Amplitude angular dependence for the case of: (a) 9, (b) 17, (c) 25, (d) 33 transducers in the star configuration for 25 mm long crack localisation

The same procedure has been repeated. Firstly, the damage maps are plotted (Fig. 12) and, as before for the 33-PZT case (Fig. 12d), the map is the most

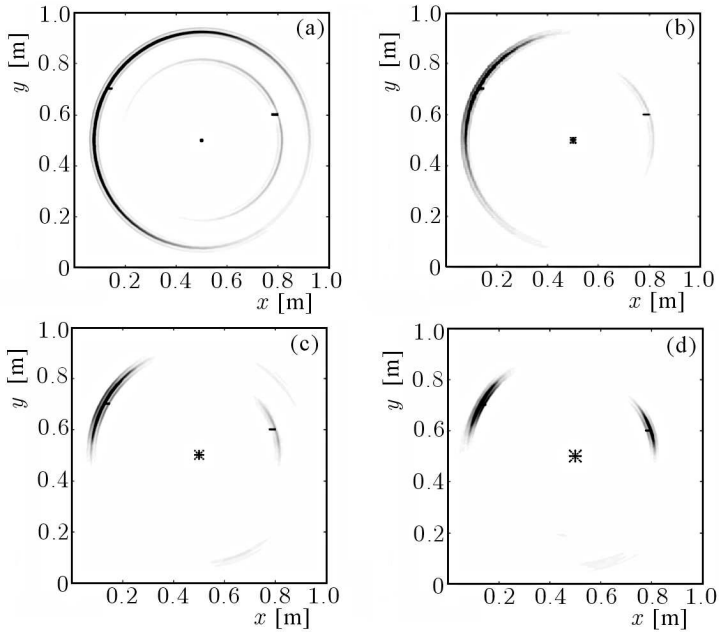


Fig. 12. Damage map for two 25mm long cracks localisation for the case of: (a) 9, (b) 17, (c) 25, (d) 33 transducers in the star configuration

precise. Especially, the second damage (on the right) is very well indicated, what cannot be said about the maps plotted for configurations with a fewer number of transducers. Secondly, the amplitude angle dependence was investigated. Figure 13 shows that only for the last configuration the direction is very well indicated. What is also important, the value of the amplitude for the second (on the right) crack is significant only for this 33-transducer configuration. The lower value of the amplitude for the second crack is a result of the crack placement in relation to the configuration. The crack on the left reflects waves better in the configuration direction than that on the right. If one placed a crack on the horizontal line for $y = 0.5$ or close to it, the reflections would not be registered by the PZTs. It is because the surface of the crack that can reflect waves back to the PZTs is very small. Surely, this should be considered as one of the disadvantages of such a concentrated configuration for damage localisation. On the other hand, one may use few concentrated configurations placed around the monitored structure to avoid areas which cannot be scanned by one configuration due to damage orientation. Another solution is the use of a distributed configuration. Then, single transducers are placed around the whole structure. This last approach needs also a localisation algorithm but this

is not the subject of this paper. Last information carried by polar plots Fig. 11 and Fig. 13 which have to be taken into consideration is the maximum level of the amplitude for each case. For one crack scenario, the amplitude decreases with the increasing number of transducers in the configuration. However, the area with this level of amplitude is wide and the amplitude drops near the direction of 45° (Fig. 11). It does not happen when 33 PZTs are used. Considering the two-crack case, the amplitude level is the highest when 33 PZTs are used and, as it was mentioned, only then the second damage is significantly indicated.

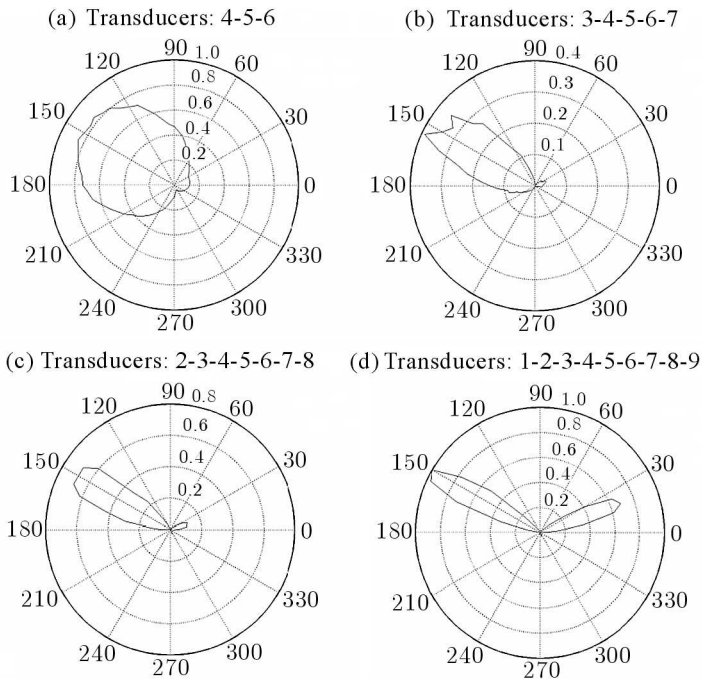


Fig. 13. Amplitude angular dependence for the case of: a) 9, (b) 17, (c) 25, (d) 33 transducers in the star configuration for two 25mm long cracks localisation

## 7. Conclusions

The phased array technique for damage localisation was successfully used. The influence of different number of transducers on damage localisation was investigated. Damage maps and polar plots were used to determine the influence of the number of transducers on damage localisation ability of the star configu-

ration. Star configurations with 9, 17, 25 and 33 transducers were compared. The best results were obtained for the 33-PZT case. Decreasing the number of transducers, results in an imprecise crack localisation and, for two cracks, in a weak response on the damage map for the second crack.

It was not attempted to continue with increasing the tnumber of ransducers, because the increase from 9 to 33 is already a large one considering the cost of transducers and necessary equipment.

Experimental verification of the proposed configuration and algorithm is planned. The size of the whole configuration will be then increased because the size of transducers will have to be taken into consideration, and it will not be possible to place them so close as the nodes in the used numerical model. The best choice seems to be to place them equally spaced. In Giurgiutiu and Bao (2004) the authors suggest that the distance should be chosen as an integer multiple of the half of the wavelength. In an experimental work, also the second propagating fundamental mode $S_0$ and the mode conversion at defects and boundaries will have to be taken into consideration.

## References

1. Deutsch W.A.K., Cheng A., Achenbach J.D., 1997, Self-focusing of Rayleigh waves and Lamb waves with a linear phased array, *Research in Nondestructive Evaluation*, **9**, 81-95
2. Fomme P., Wilcox P., Lowe M., Cawley P., 2004, Development of a permanently attached guided ultrasonic waves array for structural integrity monitoring, *Proc. 16th World Conference on NDT*, CD-ROM
3. Giurgiutiu V., Bao J., 2004, Embedded-ultrasonic structural radar for in-situ structural health monitoring of thin-wall structures, *Structural Health Monitoring, An International Journal*, **3**, 121-140
4. Greve D.W., Neumann J.J., Nieuwenhuis J.H., Oppenheim I.J. and Tyson N.L., 2005, Use of Lamb waves to monitor plates: experiments and simulations, *Proc. Sensors and Smart Structures Technologies for Civil, Mechanical, and Aerospace Systems*, **5765**, 281-292
5. Shi-Chang W., Yijun S., 1999, Optimum beam steering of linear phased arrays, *Wave Motion*, **29**, 245-265
6. Sundararaman A., Adams D.E., Rigas E.J., 2005, Biologically inspired structural diagnostics through beamforming with phased transducers arrays, *International Journal of Engineering Science*, **43**, 756-778
7. Peil U., Loppe S., 2006, Detection of structural changes by means of piezo disc, *Proc. Third European Workshop on Structural Health Monitoring*, 133-140

8. Pena J., Melguizo C.P., Martinez-Ona R., Ullate Y.G., de Espinosa Freijo F.M., Kawiecki G., 2006, Advanced phased array system for structural damage detection, *Proceedings of the Third European Workshop on Structural Health Monitoring*, 244-250

9. Purekar A.S., Pines D.J., 2001, Interrogation of beam and plate structures using phased array concepts, *Proc. of 12th International Conference on Adaptive Structures and Technology*, 275-288

10. Ye Lu, Lin Ye, Zhongqing Su, 2006, Crack identification in aluminium plates using Lamb wave signals of a PZT sensor network, *Smart Materials and Structures*, **15**, 839-849

11. Yu L., Giurgiutiu V., 2005, Advanced signal processing for enhanced damage detection with piezoelectric wafer active sensors, *Smart Structures and Systems*, **1**, 185-215

12. Zak A., Krawczuk M., Ostachowicz W., Kudela P., Palacz M., 2006, Elastic wave propagation in a cracked isotropic plate, *Proceedings of the Third European Workshop on Structural Health Monitoring*, 316-323

13. Zhongqing Su, Lin Ye, Ye Lu, 2006, Guided Lamb waves for identification of damage in composite structures: A review, *Journal of Sound and Vibration*, **295**, 753-780

## Układ fazowy przetworników w lokalizacji uszkodzeń z wykorzystaniem metody propagacji fal sprężystych

Sreszczenie

W artykule przedstawiono propozycję użycia przetworników piezoelektrycznych oraz metody propagacji fal sprężystych do lokalizacji uszkodzeń w cienkich płytach wykonanych ze stopu aluminium. Generowane fale sprężyste za pośrenictwem przetworników piezoelektrycznych, propagując w płycie, odbijają się od jej krawędzi oraz wszelkich nieciągłości. Ze względu na małe wartości amplitud fal odbitych od nieciągłości zaproponowano użycie układu fazowego przetworników do wzmocnienia sygnałów fal odbitych.

Układy fazowe wykorzystują zjawisko interferencji fal sprężystych. Zaproponowana została konfiguracja przetworników wykorzystująca cztery liniowe układy fazowe. Mapa uszkodzeń tworzona jest poprzez połączenie map składowych otrzymanych dla poszczególnych układów liniowych.

Dokonano również analizy wpływu ilości przetworników piezoelektrycznych na wyniki lokalizacji uszkodzeń. Przeprowadzone badania mają charakter wyłącznie numeryczny.

*Manuscript received February 4, 2008; accepted for print February 25, 2008*